Original paper

Ar–Ar Geochronology and Sr–Nd–Pb–O Isotopic Systematics of the Post-collisional Volcanic Rocks from the Karapınar–Karacadağ Area (Central Anatolia, Turkey): An Alternative Model for Orogenic Geochemical Signature in Sodic Alkali Basalts

Gülin GENÇOĞLU KORKMAZ[1*], Hüseyin KURT[1], Kürşad ASAN[1], Matthew LEYBOURNE[2]

[1] *Konya Technical University, Faculty of Engineering and Natural Sciences, Department of Geological Engineering, 42250, Konya, Turkey; ggkorkmaz@ktun.edu.tr*
[2] *Queen's University Department of Geological Sciences and Geological Engineering, K7L 3N6 Kingston, Ontario, Canada*
[*] *Corresponding author*

The Plio–Quaternary post-collisional volcanism in the Karapınar area is represented by two occurrences: (1) Karacadağ Volcanic Complex (KCVC) and (2) Karapınar Volcanic Field (KPVF). The investigated volcanic units are the southwestern part of the Neogene to Quaternary Cappadocia Volcanic Province (CVP) in Central Anatolia. The CVP generally displays calc–alkaline affinity in the Late Miocene to Pliocene rocks, but both calc-alkaline and sodic alkaline affinity in the Plio–Quaternary rocks, all of which have an orogenic geochemical signature. Such a volcanic activity contradicts the Western and Eastern Anatolian volcanism characterized by anorogenic OIB-like sodic alkaline volcanic rocks postdating early orogenic calc–alkaline ones. We hypothesize that such temporal and geochemical variations in the investigated rocks result from crustal contamination and present major and trace element chemistry and Sr–Nd–Pb–O isotope geochemistry, coupled with $^{40}Ar/^{39}Ar$ geochronology data to restrict the genesis and evolution of the rocks. The Neogene Karacadağ volcanic rocks are represented by lava flows, domes and their pyroclastic equivalents constituting a stratovolcano, and dated by new $^{40}Ar/^{39}Ar$ ages of 5.65 to 5.43 Ma. They are mainly composed of andesitic, rarely basaltic, dacitic and trachytic rocks and have a calc–alkaline character. Constituting a monogenetic volcanic field, the Quaternary Karapınar volcanic rocks are typically formed by cinder cones, maars and associated lavas, including xenoliths and xenocrysts plucked from the Karacadağ rocks. They comprise basaltic to andesitic rocks with a transitional affinity, from sodic alkaline to calc–alkaline. Both the Karacadağ and Karapınar volcanic rocks display incompatible trace element patterns rather characteristic for orogenic volcanic rocks. The Sr, Nd and Pb isotopic systematics of both units show a relatively narrow range, but their $\delta^{18}O$ values are markedly different. The Karacadag volcanic rocks have $\delta^{18}O$ values ranging from 7.5 to 8.9 ‰, resembling those of subduction-related basalts, but the Karapınar volcanics have $\delta^{18}O$ ratios between 5.7 and 6.5 ‰ corresponding to OIB-like rocks. Additionally, $\delta^{18}O$ values and $^{87}Sr/^{86}Sr$ ratios correlate positively with SiO_2 in the rocks, indicating that contamination played an important role during differentiation processes. All the data obtained suggest that the Karacadağ basaltic rocks stemmed from a subduction-modified lithospheric mantle source. On the other hand, the origin of the Karapınar basaltic rocks can be explained in terms of OIB-like melts contaminated with the Karacadağ volcanic rocks to gain orogenic geochemical signature, which may be an alternative model for the origin of the CVP sodic alkali basalts.

Keywords: contamination, geochronology, isotope geochemistry, post-collisional, OIB
Received: 13 January 2021; accepted: 5 April 2022; handling editor: V. Rapprich
The online version of this article (doi: 10.3190/jgeosci.343) contains supplementary electronic material.

1. Introduction

Two successive and contrasting volcanic suites in post-collisional geological settings are *orogenic* and *anorogenic* types. Orogenic volcanic suites are characterized by various rock types such as tholeiitic, calc–alkaline, shoshonitic and ultrapotassic rocks ranging from basaltic to felsic compositions, while anorogenic ones include mainly sodic alkali basaltic rocks and their differentiates (Bonin 2004). Orogenic geochemical signature (e.g., enrichment in large ion lithophile elements – LILE; K, Rb, Ba, Pb, Sr, and Th) accompanied by depletion in high field strength elements – HFSE (Nb, Ta, Ti) similar to "volcanic arc basalts" in post-collisional volcanic rocks can be related to the derivation from lithospheric mantle source metasomatically enriched by previous subduction or the effect of crustal assimilation of mantle-derived magmas during the ascent of the magma toward the surface (Pearce 1983; Pearce and Peate 1995). In an orogenic setting, the crustal component can be added by

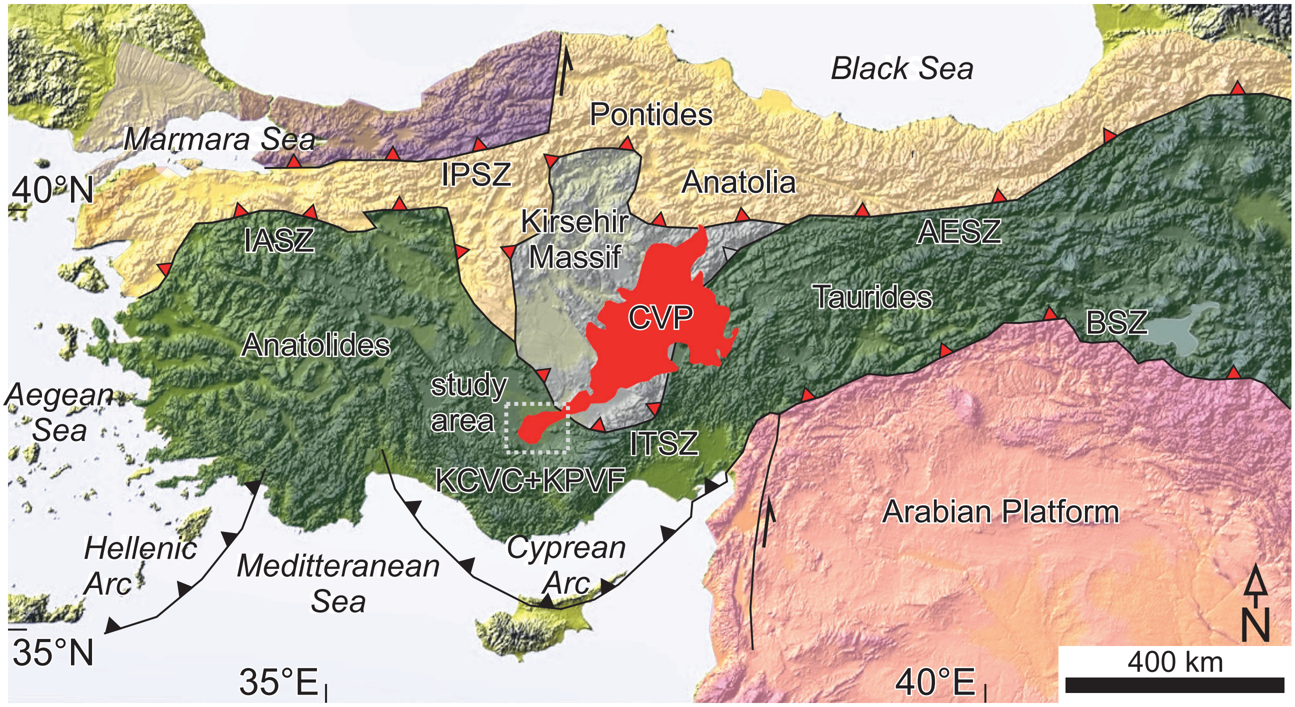

Fig. 1. Location of the Karacadağ Volcanic Complex and Karapınar Volcanic Field in the map showing the main tectonic units of Turkey (Okay and Tüysüz 1999). The map also shows the position of the Hellenic arc, as well as Cyprus arc. CVP: Cappadocian Volcanic Province, IASZ: İzmir–Ankara Suture Zone, AESZ: Ankara–Erzincan Suture Zone, IPSZ: Intra–Pontide Suture Zone, ITSZ: Inner Tauride Suture Zone, BSZ: Bitlis Suture Zone. Solid lines stand for major suture zones (black lines with red triangles) separating continental blocks and arc systems (black lines with black triangles).

two processes *via* "source contamination" in the mantle or "crustal contamination" during magma evolution. Although distinguishing the role of these two processes is difficult when true primary mantle-derived melts are absent, crustal contamination can be simply recognized by (1) the presence of crustal xenocrysts and xenoliths, (2) correlations between indices of differentiation and isotopic compositions and (3) significant variations in oxygen isotope ratios (Gertisser and Keller 2000; Peccerillo et al. 2004; Davidson and Wilson 2011; Jung et al. 2011). Conversely, anorogenic geochemical signature (e.g., peak at Nb–Ta with a trough at Pb and K on spider diagrams, similar to "OIB – oceanic island basalts") is a typical for magmas those derived from mantle source not influenced by subduction-related processes (Hofmann 1986, 1988, 1997; Hofmann et al. 1986).

Orogenic and anorogenic volcanic rock associations are characteristics of the Alpine–Mediterranean region (e.g., Betic–Alboran–Rif province, Central Mediterranean, Alps, Carpathian–Pannonian region, Dinarides and Rhodopes, Aegean sea and Anatolia) as a result of the Late Cretaceous–Cenozoic convergence of Afro–Arabian with Eurasian plates, and there is general agreement on the temporal sequence from early orogenic to late anorogenic volcanic activity in this region, except for some occurrences (Wilson and Bianchini 1999; Harangi et al. 2006; Lustrino and Wilson 2007). As a part of the Alpine–Mediterranean region, the Anatolian Late Cenozoic volcanism is traditionally reviewed in three sub-regions (e.g., Western, Central and Eastern Anatolian volcanism). Despite some overlap or opposite situations, there is a gradual transition from early orogenic calc–alkaline to potassic volcanic activity to late anorogenic sodic alkaline activity in the Western and Eastern Anatolia (Pearce et al. 1990; Güleç 1991; Aldanmaz et al. 2000; Aldanmaz 2002; Innocenti et al. 2005; Ersoy et al. 2012; Di Giuseppe et al. 2018a) as in the other Alpine–Mediterranean sectors. In contrast to the Western and Eastern Anatolia, the sodic alkali basaltic volcanic activity postdating or coeval with the orogenic calc–alkaline one is interestingly characterized by orogenic geochemical signature in Central Anatolia (Ercan et al. 1990; Reid et al. 2017; Di Giuseppe et al. 2018b; Dogan-Kulahci et al. 2018). Such a distinct signature in the Cappadocia Volcanic Province of Central Anatolia has recently been explained by mixing between subduction-related calc–alkaline and within-plate OIB-like magmas during their rise to the surface (Di Giuseppe et al. 2018b). In this scenario, crustal contamination was thought to have a negligible effect on the evolution of less evolved (basaltic) magmas. However, we hypothesize here, based on the petrography (e.g., presence of crustal xenoliths and xenocrysts, disequilibrium textures etc.) and geochemistry (e.g., crust-like trace element and isotopic signature; high LILE contents and

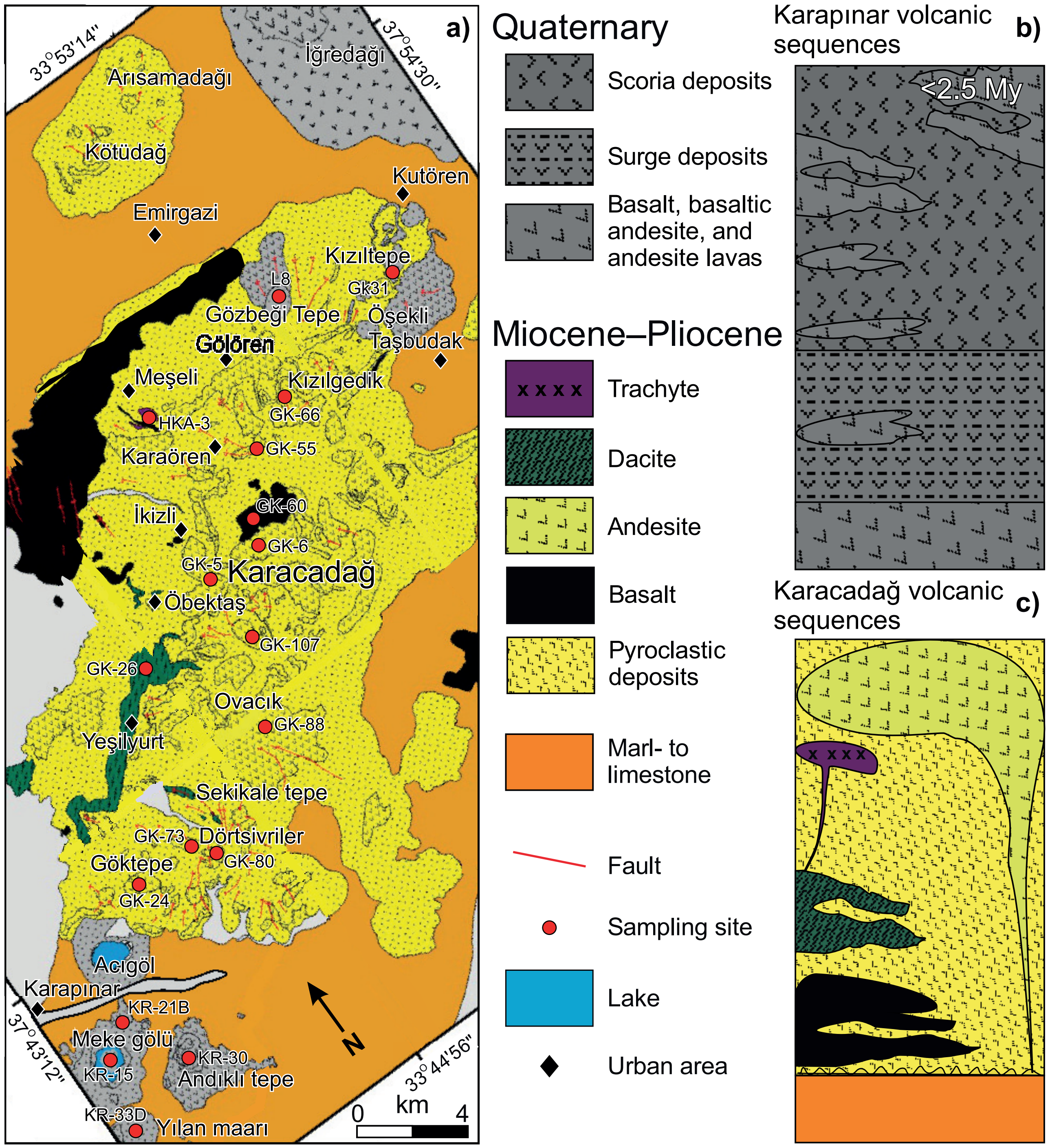

Fig. 2. a – Simplified geological map of the investigated volcanic units modified from Ulu (2009), **b** – generalized stratigraphy of the Karacadağ Volcanic Complex, and **c** – Karapınar Volcanic Field. Ages for the Karapınar volcanic rocks are from Reid et al. (2017).

high Sr, Pb, O isotope ratios, low HFSE contents and low Nd isotope ratios) of the studied volcanic rocks, that the crustal contamination is a crucial magmatic process and could be an alternative model for explaining the orogenic signature of sodic alkaline basalts from the Cappadocia Volcanic Province (CVP).

Here, we report new Ar–Ar geochronology, whole-rock major-trace element, and Sr–Nd–Pb–O isotope data from the Plio–Quaternary post-collisional volcanic rocks from the Karapınar–Karacadağ area, southwestern part of the Cappadocia Volcanic Province (Central Anatolia, Turkey). The data used in this paper is based on the results of the unpublished PhD thesis of the first author, complemented with some previously published data to strengthen the presented model.

2. Geological Setting and Volcanism in the CVP

As a part of the Cenozoic Alpine–Himalayan orogenic belt, Anatolia was formed by the combination of several tectonic blocks, and its geology was mainly shaped by the convergence system between the Afro–Arabian and Eurasian Plates. The tectonic units separated by the Neotethys sutures are "the Pontides" along the north, "the Kırşehir Block" in the middle, "the Anatolide–Tauride Block" along the south and "the Arabian Platform" in the southeast (Fig. 1). These sutures are the result of the closure of the different branches of the Neotethys Ocean by northward subduction after the Late Cretaceous (Okay and Tüysüz 1999; Okay 2008; Şengör et al. 2019). The İzmir–Ankara–Erzincan and Inner Tauride Sutures were formed by the complete closure of the Northern branch of the Neotethys following the Eocene collision of the Tauride-Anatolide block with the Pontides and the Kırşehir Block. On the other hand, the Southern branch of the Neotethys has indicated diachronous closing (Şengör et al. 2003). This branch was subducted entirely in the east, and the Arabian Platform collided with the Anatolides–Tauride Block along to the Bitlis Suture Zone at the end of the Middle Miocene. However, it is still subducting under the Anatolide–Tauride Block along to the contemporary Cyprus subduction zone in the Mediterranean.

The Cappadocia Volcanic Province (CVP) straddles the Inner Tauride Suture separating the Kırşehir and Anatolide–Tauride blocks in the Central Anatolia and is characterized by a number of monogenetic (i.e., maars, domes and cinder cones) and polygenetic volcanoes (such as Hasandağı, Karacadağ, Melendiz, Keçiboyduran and Erciyes stratovolcanoes, etc.), containing widespread ignimbrite areas of Neogene to Quaternary age (Toprak 1998). Inferred from the published radiometric data and their stratigraphy, the oldest volcanic units can be dated back to 14–13 Ma. Yet the youngest ages taken mainly from monogenetic volcanoes suggest that volcanic activity continued to the historical times in the CVP (Innocenti et al. 1975; Besang et al. 1977; Batum 1978; Ercan et al. 1992; Bigazzi et al. 1993; Notsu et al. 1995; Platzman et al. 1998; Temel et al. 1998; Le Pennec et al. 2005; Aydar et al. 2012; Lepetit et al. 2014; Reid et al. 2017; Di Giuseppe et al. 2018b; Dogan-Kulahci et al. 2018). Several geochemical and petrological studies suggest that the CVP rocks range from basaltic to rhyolitic composition and display both calc–alkaline and sodic alkaline affinity with orogenic geochemical signature. The CVP volcanism is explained by several competitive geodynamic processes such as active subduction along the Cyprus arc, decompression melting in lithospheric mantle metasomatized by the previous subduction under extensional or transtensional tectonic regime, rollback and/or foundering of the Cyprus slab (Faccenna et al. 2001; Govers and Wortel 2005; Faccenna et al. 2006; Biryol et al. 2011; Cosentino et al. 2012; Schildgen et al. 2012; Schleiffarth et al. 2018; Aydar et al. 2013; Reid et al. 2017; Di Giuseppe et al. 2018b; Dogan-Kulahci et al. 2018; Rabayrol et al. 2019). Taken as a whole, the CVP volcanism was mainly calc–alkaline in Neogene, yet both calc-alkaline and sodic alkaline in Quaternary based on the published geochronological and geochemical data.

The Karacadağ Volcanic Complex (KCVC) and Karapınar Volcanic Field (KPVF) are located on the southwestern edge of the CVP. The Karacadağ volcanic complex was previously named from the Karacadağ stratovolcano (Keller 1974) and is represented by intermediate to felsic lava flows, domes and their pyroclastic equivalents in Mio–Pliocene age (4.7–5.98 Ma) (Platzman et al. 1998). The pioneering study of Keller (1974) has suggested that the Karacadağ volcanic samples range from andesite to dacite with calc-alkaline affinity. Cinder cones, maar craters and associated lava flows in the study area were previously named as "the Recent Quaternary volcanoes of Karapınar" by Keller (1974), but recently termed as "Hasan Monogenetic Cluster (Reid et al. 2017)" or "Karapınar Monogenetic Field (Uslular and Gençalioğlu-Kuşcu 2019)". Here, we collected these volcanic formations under the name of "the Karapınar volcanic field" for simplification. Cinder cones overlie the Karacadağ volcanic complex on the northeast near Kutören (Fig. 2) and include ejected dacitic blocks of the Karacadağ volcano. The Karapınar basaltic to andesitic lava flows appear to have fed from fissures and contain xenoliths and xenocrysts plucked from the Karacadağ volcanic complex, which was first identified as evidence of contamination by Keller (1974). Four well-known maar craters are present in the study area, one of which has a central cinder cone in maar lake (Mekegölü). These explosion craters are characterized by base surge deposits exposed in the surrounding pyroclastic rings. Phreatomagmatic tuff-rings and cones are other common volcanic forms of the Karapınar volcanic field. Based on the published geochronology data, cinder cones and associated basaltic flows from the Karapınar monogenetic field have ages < 0.6 Ma, but they can be dated back to 2.5 Ma in the whole CVP (Notsu et al. 1995; Reid et al. 2017; Dogan-Kulahci et al. 2018). The composition of the Karapınar volcanic rocks range from basalt to andesite, and they show both (sodic) alkaline and calc–alkaline character (Keller 1974; Ercan et al. 1992; Notsu et al. 1995; Olanca 1999; Reid et al. 2017; Di Giuseppe et al. 2018b; Dogan-Kulahci et al. 2018).

3. Material and methods

Around 700 samples were collected from the lava flows, sills, domes, and pyroclastic deposits in the study area for petrographic, geochemical and geochronological investi-

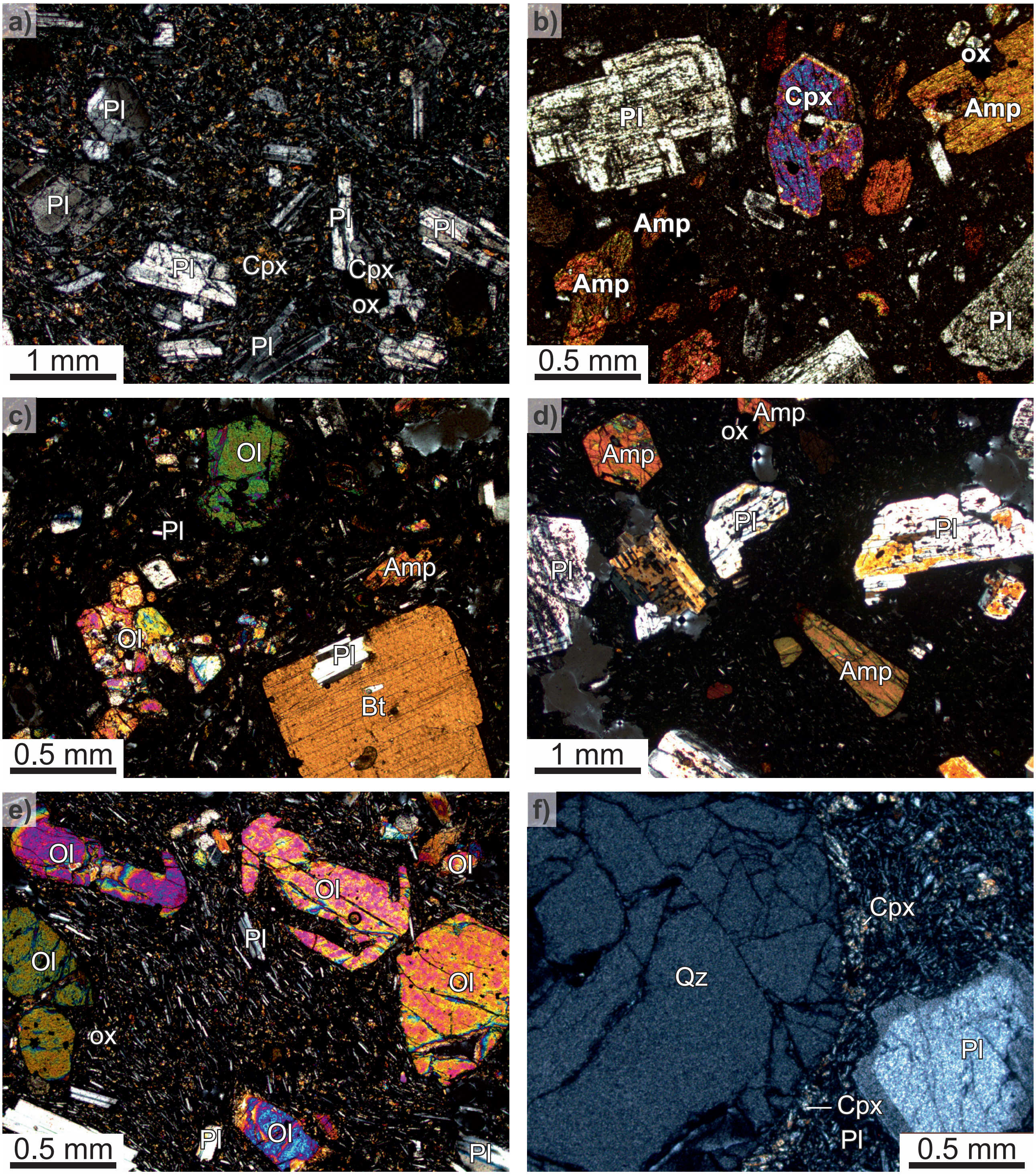

Fig. 3. Microphotographs of the Karapınar-Karacadağ volcanic rocks **a** – fine and dusty sieved plagioclases in hypocrystalline porphyritic B1 (Basalt-1) and **b** – hypocrystalline porphyritic A1 (Andesite-1), **c** – olivine xenocrysts in hypocrystalline porphyritic A2 (Andesite-2), **d** – coarse sieved plagioclases and bladed amphibole in hypocrystalline porphyritic D (Dacite), **e** – skeletal olivine in holocrystalline porphyritic B2 (Basalt-2), **f** – ocelli quartz and sieved plagioclase xenocrysts in B3 (Basalt-3), (Amp = amphibole; Bt = biotite; Cpx = clinopyroxene; Ol = olivine; ox= Fe–Ti oxide; Qz = quartz; Pl = plagioclase).

gations. Firstly, weathering rinds were extracted from all samples, and each was separated and carefully checked to make sure that only the freshest material possible would be further powdered and prepared for analytical work. About 180 thin sections were made in the Ankara University, Earth Sciences Application and Research

Table 1 Mineralogical compositions and the textural properties of the investigated samples from the Karapınar Volcanic Field and Karacadağ Volcanic Complex.

Volcanic Rocks	Rock Type/ Symbol	Age	Mineral composition	Texture	Enclave Types
Karacadağ Volcanic Complex	Basalt-1/B1	Neogene	Pl + Cpx + Ol + ox	Pilotaxitic, cellular and sieve (Pl)	–
	Andesite-1/A1	Neogene	Pl + Cpx + Amp + ox ± Bt ± Qz ± Ap ± Zrn	Hypocrystalline porphyric, glomeroporphyritic texture, cellular and sieve texture (Pl)	1. Magma Segregation Enclaves (Cognate xenolith) 2. Magma mixing enclaves
	Andesite-2/A2	Neogene	Pl + Cpx + Opx + Amp + Bt + Ol xe + ox ± Ap ± Zrn	Hypocrystalline porphyric, spongy cellular and sieve texture (Pl)	1. Magma Segregation Enclaves (Cognate xenolith) 2. Magma mixing enclaves
	Andesite-3/A3	Neogene	Pl + Cpx + Opx + ox ± Ap ± Zrn	Hypocrystalline porphyric, glomeroporphyritic texture, cellular and sieve texture (Pl)	1. Magma Segregation Enclaves (Cognate xenolith)
	Andesite-4/A4	Neogene	Pl + Cpx + ox	Hyalopilitic porphyric, cellular and sieve texture (Pl)	–
	Dacite/D	Neogene	Qz + Pl + Cpx + Amp + Bt + ox	Hypocrystalline porphyric, spongy cellular and sieve texture (Pl)	–
	Trachyte/T	Neogene	Pl + Sa + Cpx + Ol	Vitroporphyritic	–
Karapınar Volcanic Field	Basalt-2/B2	Quaternary	Ol + Cpx + Pl + ox (± Qz xe)	Holocrystalline porphyric, texture – hypocrystalline porphyric, glomero-porphyritic, vesicular, cellular and sieve (Pl), ocellar (Qz)	1. Magma Segregation Enclaves (Cognate xenolith) 2. Xenocrysts and xenoliths (quartzite fragments)
	Basalt-3/B3	Quaternary	Cpx + Pl + Ol + ox (Amp ± Bt ± Qz ± Pl xe)	Hypocrystalline porphyric, glomeroporphyritic, vesicular, amygdaloidal, cellular and sieve (Pl), ocellar (Qz)	1. Magma Segregation Enclaves (Cognate xenolith) 2. Magma mixing enclaves 3. Xenocrysts (Qz, Pl, Bt, Amp)

Amp – amphibole; Ap – apatite; Bt – biotite; Cpx – clinopyroxene; Ol – olivine; Opx – orthopyroxene; ox – Fe-Ti oxides; Pl – Plagioclase; Sa – sanidine; Qz – quartz; Zrn – zircon; xe – xenocryst (Mineral abbreviations after Warr 2020).

Center (YEBIM) for mineralogical and petrographical investigations. Detailed petrographical investigations were executed under a petrographic microscope and microphotographed at the Konya Technical University.

The most representative and freshest samples whose mineralogical and petrographic properties were determined were powdered in an agate ball-mill in the Ankara University YEBİM. And then, eighteen representative samples were sent to ACME laboratory (Canada) for whole-rock major, trace, and rare earth element analyses with the code of LF202. Firstly, whole-rock major element analyses were performed by the Inductively Coupled Plasma Atomic Emission Spectrometer (ICP-AES). After dissolving the samples, trace and rare earth elements were detected by Inductively Coupled Plasma Mass Spectrometry (ICP-MS). In-house standards (e.g., Reference Materials STD SO-19, STD OREAS45EA, and STD DS11) were analyzed together with the samples, and they were used for the calibration of the dataset. Whole-rock major and trace element results of the samples and Quality Control (QC) data, including the analyzed standard materials, are given in Supplementary files (ESM1). Based on replicate analyses on the reference materials, precision was evaluated to be better than 1 % for major elements except for P_2O_5 (2.5 %) and 5 % for trace and rare earth elements.

$^{40}Ar/^{39}Ar$ geochronology analyses of two samples were executed at the WiscAr Geochronology Laboratory at the University of Wisconsin–Madison (USA). To determine the cooling ages of the rocks, the freshest samples were selected from the Karacadağ volcanic complex at different locations. Ar–Ar geochronology analyses were executed on a basaltic whole-rock sample and an amphibole separation from a dacitic sample. The $^{40}Ar/^{39}Ar$ variant of conventional ^{40}K–^{40}Ar dating depends on producing some ^{39}Ar in each sample by bombarding in a nuclear reactor. After the samples are returned from the reactor, the isotopic composition of the argon is measured. When analyzing, a 25 Watt CO_2 laser can focus on spots between 10 and 400 µm in diameter. These analyses yield a plateau age at the 95% confidence level.

Isotopic ratios of Sr, Nd and Pb from four representative samples selected upon results of bulk rock geochemistry were analyzed using a Finnigan MAT262 RPQ2+ Thermal Ionization Mass Spectrometer (TIMS) at GEOMAR Helmholtz Centre for Ocean Research in Kiel (Germany). For this purpose, powder samples were prepared at Ankara University YEBİM. The powder samples were digested in a solution concentrated ultra-pure HF and HNO_3 at 150 °C for 60 h. Following the procedures of Geldmacher et al. (2006) and Hoernle et al. (1991), ion chromatography was executed. Sr and Nd isotope ratios were normalized to $^{86}Sr/^{88}Sr$ =0.1194, and $^{146}Nd/^{144}Nd$ = 0.7219, respectively. Moreover, all Pb isotope ratios were normalized to the reference ratios for USGS NBS 981 of Baker et al. (2004). External precisions are 2σ for all radiogenic isotopes.

Oxygen isotope ($^{18}O/^{16}O$) analyses of three whole-rock samples and five olivine separates were provided at the Queen's University Queen's Facility for Isotope Research (QFIR). Oxygen was extruded from 5 mg samples at 550–600 °C according to the conventional BrF5 method of Clayton and Mayeda (1963) and measured by a dual inlet on a Thermo-Finnigan Delta Plus XP Isotope-Ratio Mass Spectrometer (IRMS). $\delta^{18}O$ ratios are presented utilizing the delta (δ) notation in units of permil (‰) relative to the Vienna Standard Mean Ocean Water (VSMOW) international standard, with a precision of 0.5 ‰. Results of both radiogenic and stable isotope analyses of the samples are available in Supplementary files (ESM2).

4. Results

4.1. Petrography

Based on the petrography (Tab. 1 and Fig. 3) and geochemistry (Fig. 4), the studied rocks can be separated into several units. Karacadağ volcanic complex comprises basaltic andesites (B1), four andesite units (A1 to A4), dacites (D) and trachytes (T), whereas Karapınar volcanic field comprise two groups of basalts to basaltic andesites (B2 and B3).

The Karacadağ basaltic andesites (B1) exhibit hypocrystalline porphyritic texture with phenocrysts of plagioclase, clinopyroxene, and rare Fe–Ti oxides. Those are enclosed in a fine-grained groundmass composed of the same mineral assemblages complemented with iddingsite pseudomorphs after olivine and rare glass (Fig. 3a). However, the Karacadağ andesitic rocks show textures ranging from holocrystalline porphyritic to vitrophyric porphyritic textures, and display disequilibrium textures as cellular-sieve textured plagioclases, amphiboles, and clinopyroxenes. Andesite-1 (A1) group rocks generally contain phenocrysts of mainly clinopyroxene, amphibole, and plagioclase, rare or no biotite, quartz xenocrysts, and Fe–Ti oxides enclosed in isotropic glass (Fig. 3b). Andesite-2 (A2) group rocks differ in the common presence of biotite, with otherwise mineral assemblage similar to A1 group. This unit also includes rare quartz and olivine xenocrysts (Fig. 3c). Andesite-3 (A3) group rocks are classified as two-pyroxene andesites composed of dominantly ortho and clinopyroxene, plagioclase, and Fe–Ti oxides and minor quantities of glass. While disequilibrium and/or decompression reaction textures are present in (A3) (resorbed and sieved plagioclase,

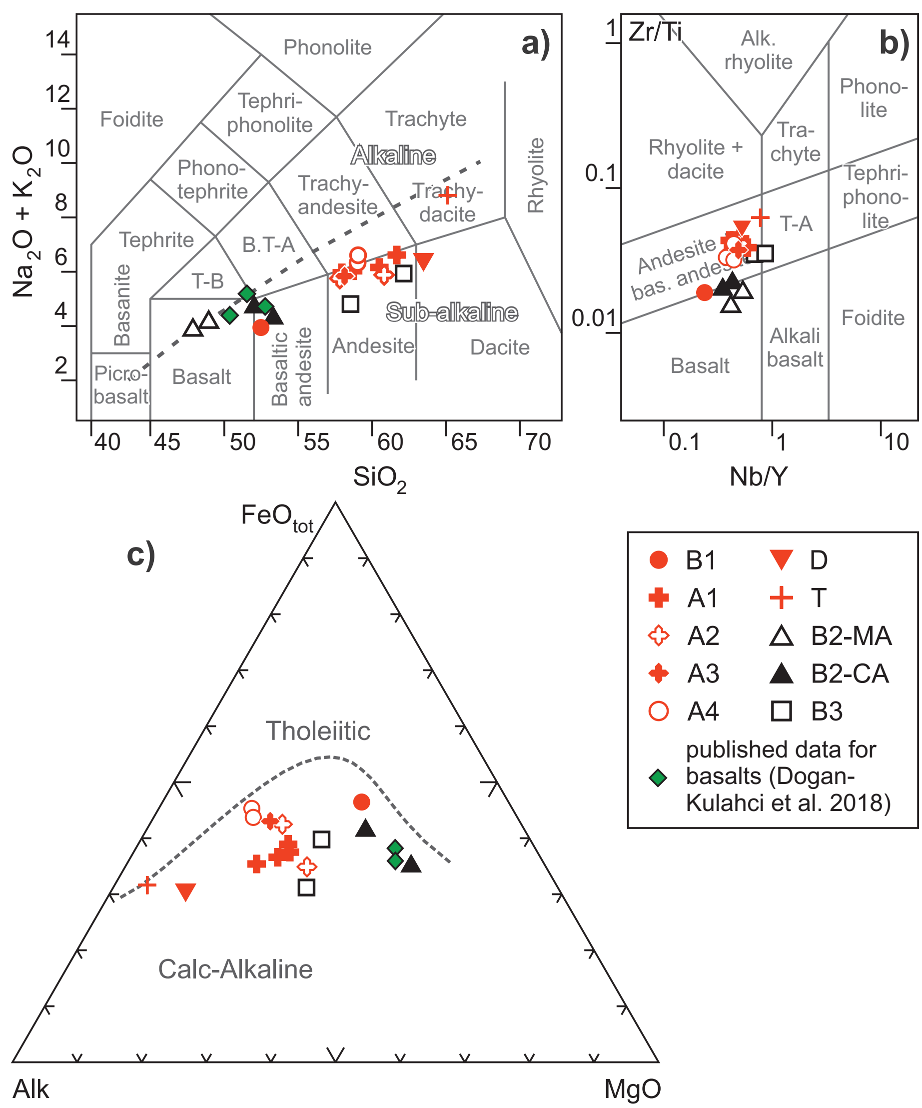

Fig. 4. a – Total alkali-silica (TAS) diagram (Le Bas et al. 1986), the red line separates alkaline and subalkaline fields according to Irvine and Baragar (1971), **b** – Nb/Y vs. Zr/Ti diagram (Pearce 1996) of the investigated rocks, **c** – AFM diagram of the subalkaline volcanic rocks (Irvine and Baragar 1971). Red symbols indicate the Karacadağ volcanic rocks, and black symbols stand for the Karapınar volcanic rocks. MA: Mildly-alkaline; CA: Calc--alkaline. Green diamonds stand for Karapınar basalts in the previous research (Dogan-Kulahci et al. 2018).

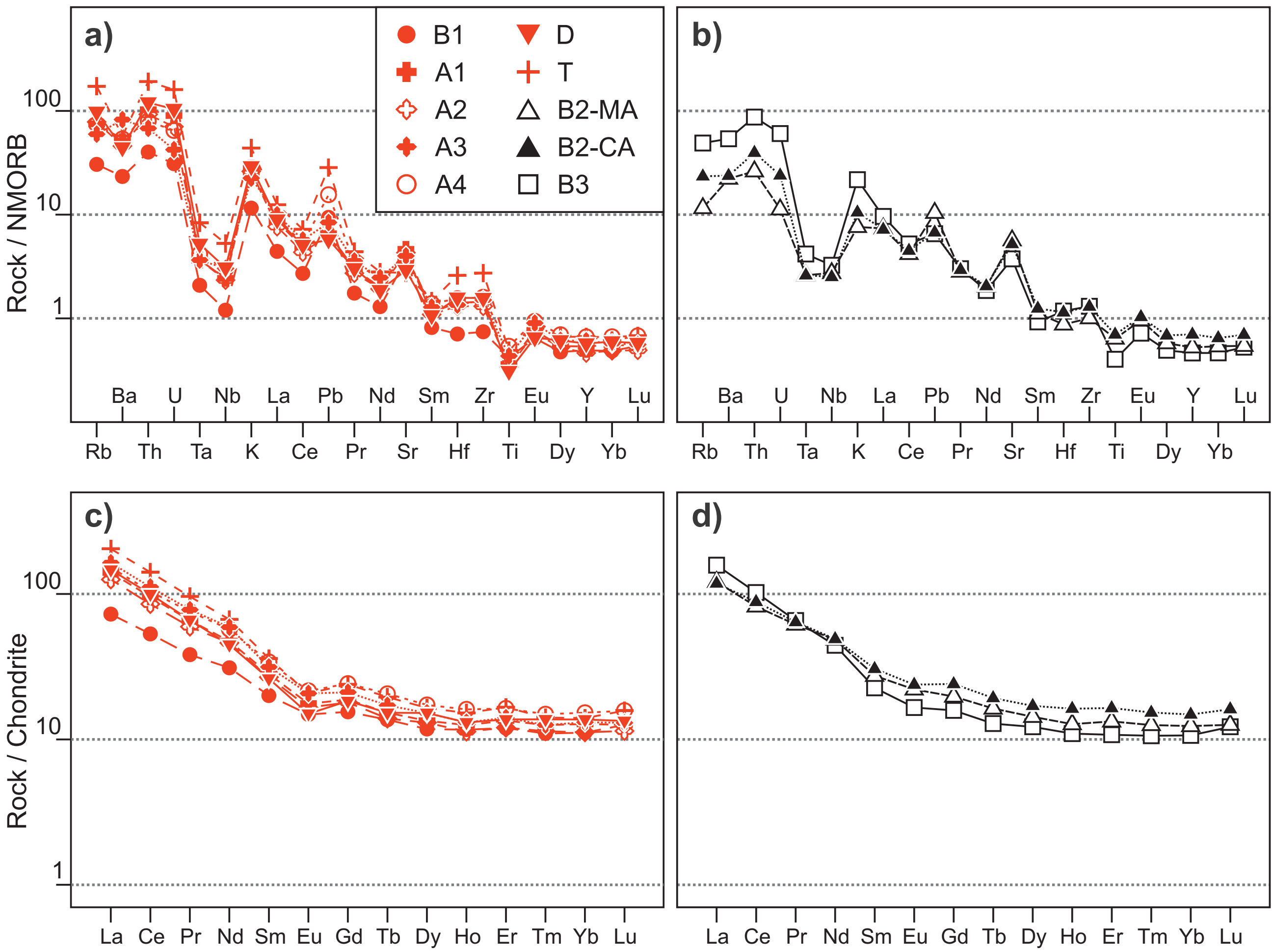

Fig. 5. a, b – MORB-normalized (Hofmann 1988) and **c, d** – Chondrite-normalized (Sun and McDonough 1989) diagrams of the most representative Karapınar-Karacadağ volcanic rocks. The symbols are the same as in Fig. 4.

plagioclase ± clinopyroxene ± Fe–Ti oxide clots), they are much less abundant than in A1 and A2 (ESM3). Andesite-4 (A4) group rocks display pilotaxitic texture and consist mainly of plagioclase and Fe–Ti oxide minerals, rarely clinopyroxene, and have microlithic groundmass (ESM3). Dacites (D) have hypocrystalline porphyritic texture, dominated by amphibole, and less frequent biotite, plagioclase, and rarely quartz and Fe–Ti oxides in a glass-rich groundmass (Fig. 3d). Trachytes (T) exhibit vitrophyric porphyritic texture and are composed mostly of plagioclase, rare clinopyroxene, sanidine, and Fe–Ti oxide minerals embedded in a glassy groundmass (ESM3). Some of the andesites from the Karacadağ rocks contain gabbroic cognate xenoliths and enclaves displaying magma mixing between basaltic and andesitic melt.

The Karapınar basalt to basaltic andesite lavas are characterized by porphyritic texture. Basalt-2 group rocks (B2) contain mainly olivine, clinopyroxene, plagioclase, and rare Fe–Ti oxides (Fig. 3e). Quartz xenocrysts occur scarcely as well. Basalt-3 group rocks (B3) differ from B2 rocks in a lower amount of olivine and a higher proportion of clinopyroxene phenocrysts accompanied by plagioclase (sieve-textured, up to 20 vol. %) and Fe–Ti oxides (ESM3). In addition, they contain common quartz xenocrysts (up to 10 %), rare biotite, and amphibole xenocrysts (Fig. 3f and ESM3). Quartz xenocrysts with corrosive embayments and also ocellar texture surrounded by clinopyroxenes. Also, amphibole and biotite minerals are completely opacitized.

4.2 Major and Trace Element Composition

The Karacadağ volcanic rocks were classified as basaltic andesite (B1), andesites (A1 to A4), dacite (D) and trachyte (T; $q < 20\,\%$), whereas the Karapınar volcanic rocks as basalt, basaltic andesite and andesite (B2 and B3) (Figs. 4a, b). The Karapınar volcanic rocks have a transitional geochemical character (calc–alkaline; CA to mildly alkaline; MA), while the Karacadağ volcanic rocks are subalkaline (Fig. 4a). In the AFM diagram (Fig. 4c),

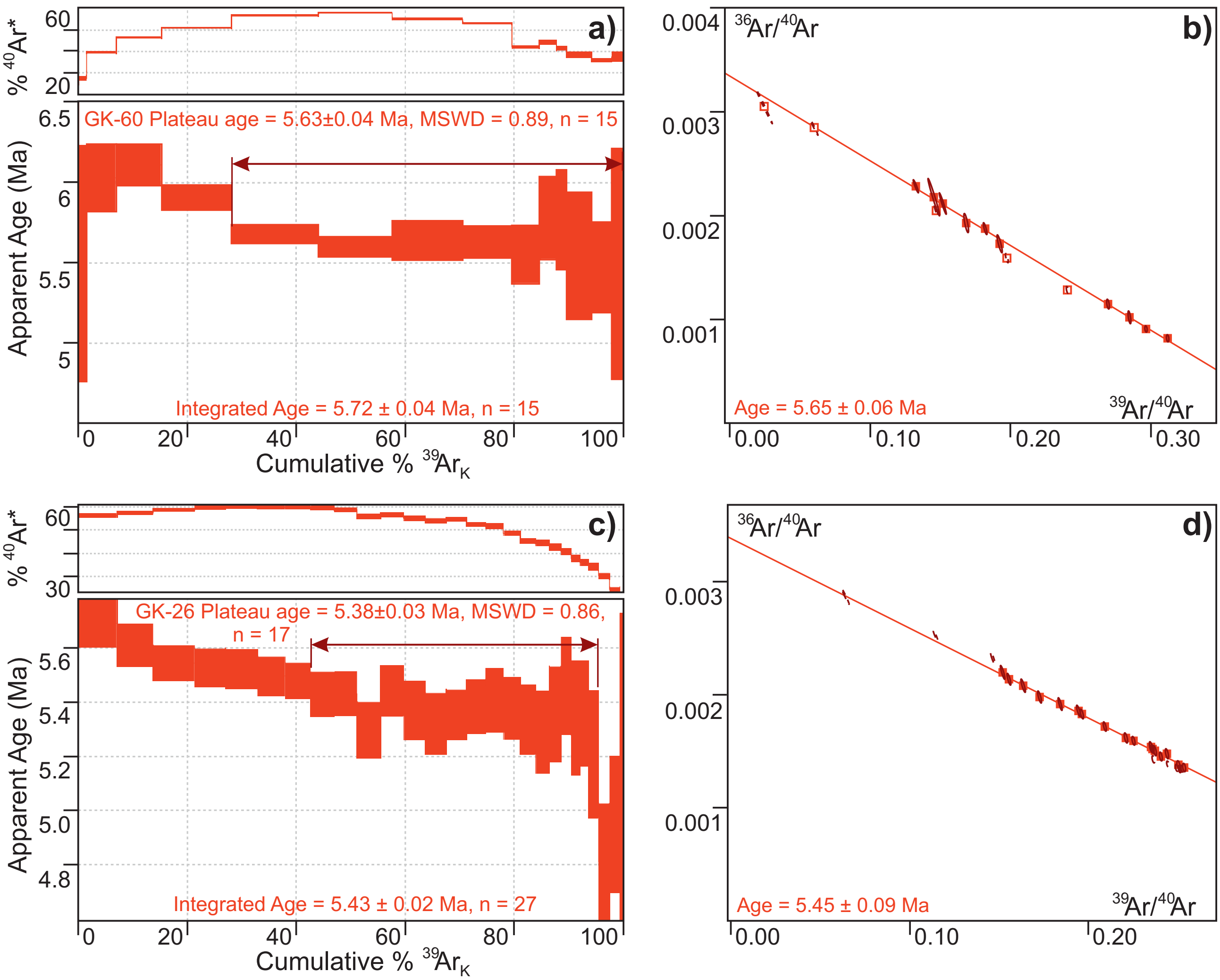

Fig. 6. **a** – ^{39}Ar/ ^{40}Ar age spectra (plateau age) and **b** –inverse isochron (isochron age) of Basalt-1 **c** – ^{39}Ar/ ^{40}Ar age spectra (plateau age) and **d** – inverse isochron (isochron age) of an amphibole mineral separate from Dacite.

all subalkaline samples plot in the calc–alkaline field. Consistently with their chemical character, mildly alkaline samples from the Karapınar rocks have normative nepheline plus olivine, but calc–alkaline samples have normative hypersthene plus quartz or olivine.

The SiO_2 *vs.* major and trace elements show variations characterized by straight linear, curved, or inflected trends with progressive differentiation for the Karapınar and Karacadağ volcanic rocks. MgO, Fe_2O_3, CaO, TiO_2, Sc, Co, Cr and V linearly decrease with increasing SiO_2, but K_2O, Rb, Ba, Zr, Th and La have a good positive correlation with SiO_2 (ESM4). On the other hand, Al_2O_3 and Sr variations show complex patterns when plotted against SiO_2. Al_2O_3 increases until SiO_2 reaches ~55 wt. %, then it decreases, but Sr linearly decreases for the Karapınar samples. Conversely, Sr increases until SiO_2 reaches ~55 wt. %, then it decreases, but Al_2O_3 linearly decreases for the Karacadağ samples. Although the Karapınar and Karacadağ samples generally display similar major and trace element variations, they plot on the different parallel trends in some diagrams (ESM4).

Basaltic rocks from the investigated suites exhibit enrichments in large ion lithophile elements (LILE; K, Ba, Rb, Sr, Pb, and Th) and light rare earth elements (LREE; La, Ce) with distinct Nb–Ta–Ti trough on the N-MORB-normalized spider diagrams (Figs 5a, b). However, the studied intermediate and felsic units exhibit patterns that are largely comparable with those of the basaltic rocks, but they are more enriched in incompatible trace elements than basaltic ones. On the chondrite-normalized rare earth element (REE) plots (Figs 5c, d), the studied rocks exhibit moderately fractionated LREE patterns (Karacadağ volcanics La_N/Yb_N =6.2–13.8, and Karapınar volcanics La_N/Yb_N = 7.54–14), and they also show flat heavy-REE (HREE) distributions. As in the spider diagrams, the intermediate and felsic rocks show more enrichment in all REEs relative to the basaltic samples. Spider and REE diagrams of the Karapınar and Karacadağ volcanic rocks resemble each other, except for distinct depletion in Ba and slight negative Eu anomaly of the Karacadağ samples. Spider diagrams also indicate that the Karapınar calc–alkaline basalts were seemed more enriched in LREE and LILE relative to the Karapınar mildly alkaline basalts.

4.3. Geochronology

^{40}Ar–^{39}Ar age data of the basalt from the Karacadağ volcanic complex is shown as apparent age in Figs 6a and 6b. Whole-rock fragments from the basalt yielded meaningful plateau age of 5.65 ± 0.06 Ma. An amphibole separate from dacites yielded ^{40}Ar–^{39}Ar plateau age of 5.379 ± 0.028 Ma and an isochron age of 5.45 ± 0.09 Ma (Figs 6c–d).

4.4. Sr-Nd-Pb-O Isotope systematics

The Karacadağ (B1) and Karapınar (B2) basalts have positive εNd (t: 5.65 Ma) values of 1.67 to 9.02 and $^{87}Sr/^{86}Sr$(i) ratios in the range 0.70491–0.70518 (ESM2; Fig. 7). The investigated intermediate-acidic rocks from the Karacadağ volcanic complex are characterized by negative εNd values from –1.21 to –2.29 and $^{87}Sr/^{86}Sr$(i) ratios 0.705188–0.70635. The investigated rocks show limited variations in Pb isotope ratios with $^{206}Pb/^{204}Pb$ = 18.88–18.93, $^{207}Pb/^{204}Pb$ = 15.72–15.66, and $^{208}Pb/^{204}Pb$ = 39.03–38.17 (ESM2; Fig. 8). Generally, the olivine grains separated from the Karapınar volcanic rocks vary in $\delta^{18}O$ between 5.7 and 6.5 ‰ (ESM2). However, Karacadag volcanic rocks have $\delta^{18}O$ values ranging between 7.5 and 8.9. The $\delta^{18}O$ values of the Karacadağ whole-rock samples (7.7–8.9 ‰) are much higher than those of the olivine separates (7.5 ‰).

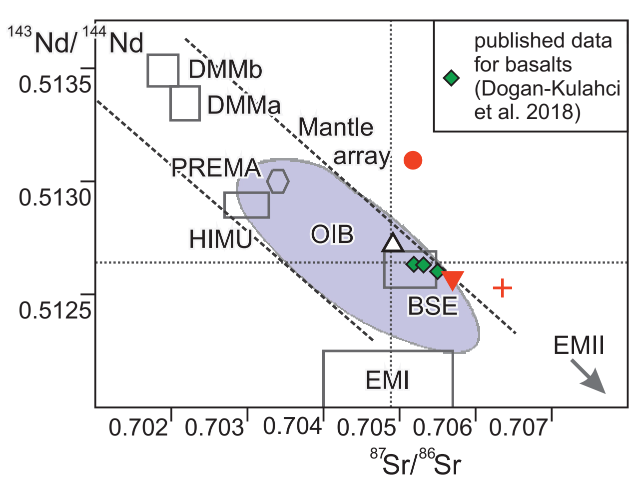

Fig. 7. Sr–Nd isotope correlation diagram (Zindler and Hart 1986) (BSE: Bulk Silicate Earth, DMM: depleted mantle, EMI/EMII: enriched mantle, HIMU = high $^{238}U/^{204}Pb$ mantle, OIB: ocean island basalts, PREMA: prevalent mantle). The symbols are the same as in Fig. 4.

5. Discussion

5.1. Fractional Crystallization vs. Magma Mixing

Major and trace element variation diagrams (ESM4) give valuable information on the fractionated phases during fractional crystallization. Therefore, the decrease of MgO, CaO, Ni and Cr with increasing SiO_2 can be best clarified by olivine and clinopyroxene fractionation, especially in the basaltic rocks. The decrease in Fe_2O_3, TiO_2, Sc, Co and V shows the crystallization of Fe–Ti oxides (e.g., magnetite, ilmenite etc). Although Al_2O_3 and Sr variations are complex, they can be interpreted by plagioclase accumulation in the basaltic rocks but its fractionation in the evolved rocks. Other information on the fractionated phases may be taken from REE patterns of the investigated rocks. The slight depletion in MREE of the Karacadağ intermediate to felsic rocks can be attributed to the amphibole fractionation in their evolution because amphibole preferentially incorporates MREE relative to the LREE and HREE, especially in the evolved rocks (Davidson et al. 2007). On the other hand, the Karacadağ intermediate to felsic rocks show a slight negative Eu anomaly in their REE patterns, indicating the role of plagioclase fractionation in the evolution of the rocks. Although the Karapınar and Karacadağ samples generally exhibit similar major and trace element variations, and they follow different trends in SiO_2 vs. Al_2O_3, K_2O, Zr, V, Cr, La, Rb, and Sr diagrams (e.g., ESM4), suggesting a distinct differentiation history.

The investigated rocks, especially intermediate ones, show disequilibrium textures and mineralogies with various enclave types and linear trends in some major and trace element distribution plots. These are suggestive of magma mixing. To test the role of magma mixing in the evolution of the volcanic units, we performed mixing models (Bryan et al. 1969) based on the least-squares regression of the major and trace elements for a subset of the intermediate samples by using IgPet. Based on about twenty calculations, we tested the mixing combination of the basaltic and felsic end members from the KPVF and KCVC to be able to produce an intermediate composition. In such models, $\sum r^2$ (e.g., the sum of squares of residuals; a measure of the differences between calculated and observed element abundances), is anticipated to be low, approximating zero for acceptable models. The high $\sum r^2$ of our calculations suggests that magma mixing is not a dominant magmatic process in the evolution of the modeled intermediate units. To sum up, we stress here that fractional crystallization played a major role relative to magma mixing in the evolution of the investigated rocks.

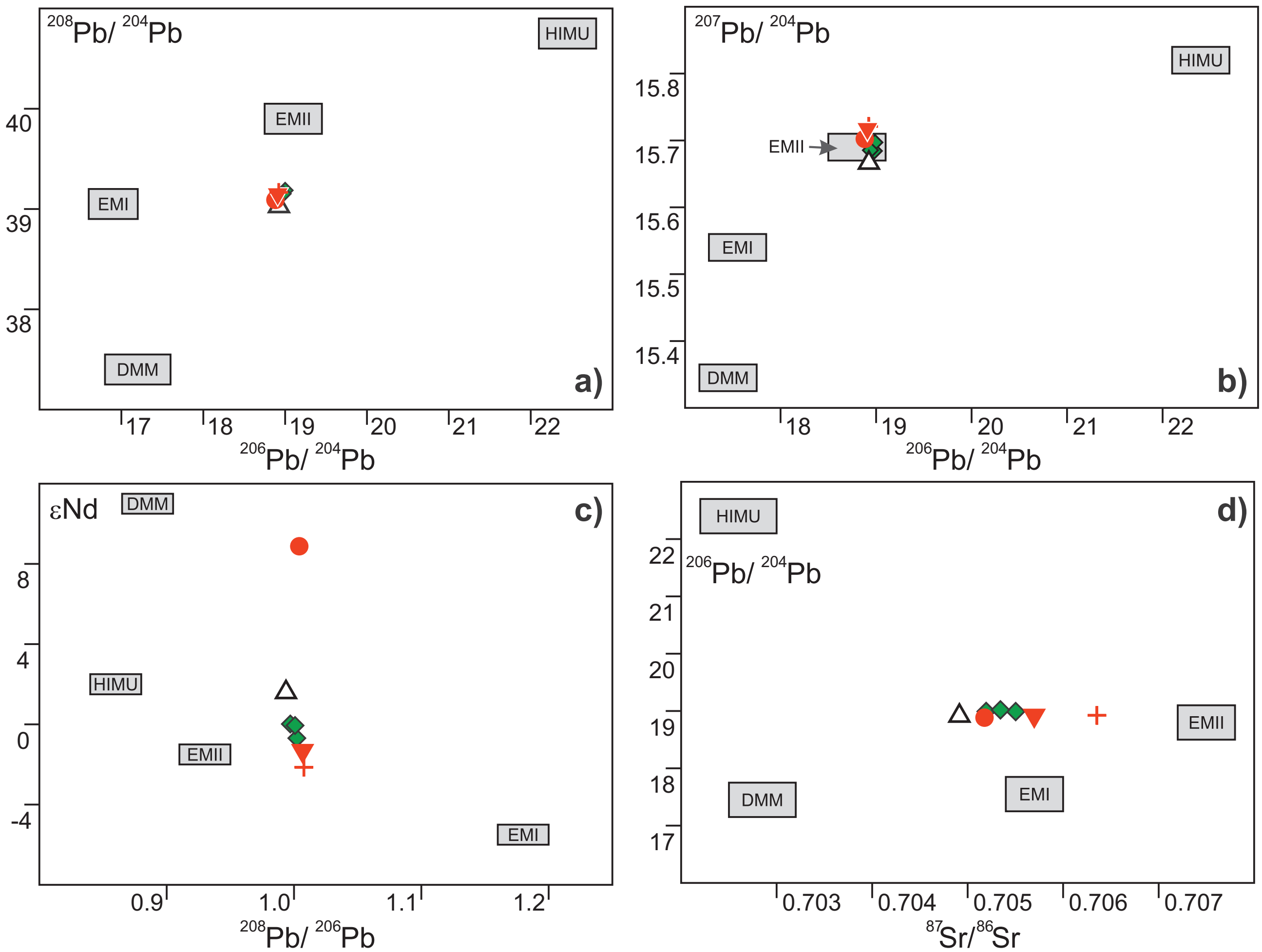

Fig. 8. **a** – ^{206}Pb/^{204}Pb-^{207}Pb/^{204}Pb, **b** – ^{206}Pb / ^{204}Pb-^{208}Pb/^{204}Pb **c** – ^{206}Pb/^{204}Pb-eNd and **d** – ^{87}Sr-^{86}Sr-^{206}Pb/^{204}Pb isotope diagrams of investigated volcanic rocks Isotope compositions of mantle sources DMM, EMI, EMII, HIMU after Hofmann (2007). The symbols are the same as in Fig. 4.

5.2. Crustal vs. Source Contamination

N-MORB-normalized spider diagrams of the investigated basaltic rocks exhibit enrichments in large ion lithophile elements (LILE: Ba, K, Rb, Sr, Pb, and Th) and light rare earth elements (LREE, namely La, Ce) with distinct Nb–Ta–Ti trough, which is typical for volcanic rocks at convergent margins. Many researchers have suggested that mantle source contamination by subduction-related processes and crustal contamination were possible for the genesis and evolution of the Neogene CVP calc–alkaline rocks, including the Karacadağ volcanic rocks. However, the transitional Quaternary Karapınar volcanic rocks cannot be originated from a mantle source contaminated by subduction-related processes because the Karapınar basaltic rocks have δ^{18}O values and incompatible trace element ratios resembling those of OIB-like volcanic rocks, which will be further discussed.

Nb/U, Ce/Pb and Nb/Ta are considered useful indicators to assess the effect of crustal contamination on basaltic rocks (Rudnick and Gao 2003; Dai et al. 2018). B1 has Ce/Pb (~7) and Nb/U (~2) ratios having crustal signature (Ce/Pb:~4), Nb/U: 10; Hofmann 1986). On the other hand, B2 and B3 group rocks have Ce/Pb ratios (~8–16 and 20, respectively), close to those for OIB (~25), while their Nb/U ratios (2–12 and 3, respectively) are lower than OIB (~47) (Hofmann et al. 1986; Tab. 2; ESM5). Moreover, the investigated basaltic rocks are represented by different Nb/Ta ratios. B1 exhibits Nb/Ta ratios (10.5) resembling those for the continental crust

Table 2 Some trace element ratios of the basalts from the Karapınar Volcanic Field and Karacadağ Volcanic Complex.

Sample		Ce/Pb	Nb/U	Nb/Ta	Th/Yb
Basalt-1	GK60	7.07	1.91	10.50	3.96
Basalt-2	GK31*	14.81	9.89	14.83	1.90
	L8*	9.84	12.00	19.20	2.33
	KR21B_E.	7.98	3.74	17.20	3.88
	KR15	16.36	5.18	17.60	2.93
Basalt-3	KR30	19.56	2.65	14.25	9.00
	KR-33D	5.08	0.77	15.05	8.85

* – Mildly alkaline (ne-normative) basalts

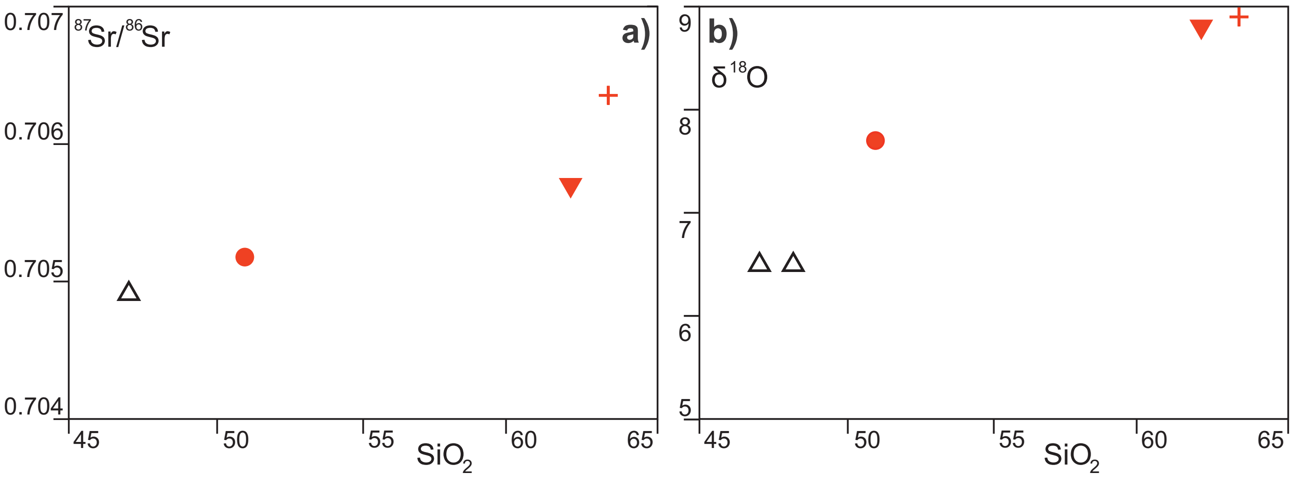

Fig. 9. SiO_2 vs. $^{87}Sr/^{86}Sr$ **a** – and $\delta^{18}O$ **b** – variations of the representative KPVF and KCVC rocks.

(12: Pfänder et al. 2012). However, B2 samples have Nb/Ta ratios (17–19.2), which are specific for the chondrites (19.9; Münker et al. 2003), and B3 group rocks (Nb/Ta = 14–15) have OIB-like signature (14: Pfänder et al. 2012). Furthermore, the enrichment of Th/Yb ratios relative to SiO_2 and Nb/Yb can be attributed to crustal contamination (Kheirkhah et al. 2015; ESM5). Based on the trace element ratios, we suggest that crustal contamination had a key role in the evolution of the studied volcanic units and was more effective in the evolution of the Karacadağ volcanic rocks relative to the Karapınar volcanic rocks.

Alteration and low-temperature weathering after a volcanic eruption can increase the $\delta^{18}O$ of the rocks. Therefore, the isotope value of the mantle source is represented by the $^{18}O/^{16}O$ values of the mineral separations rather than those of the whole-rock (Davidson and Harmon 1989; Ellam and Harmon 1990; Downes et al. 1995; Dobosi et al. 1998). Whole-rock $\delta^{18}O$ values of the investigated rocks (7.7–8.9 ‰) are slightly higher than those of the olivine grains (7.5 ‰). Whole-rock $\delta^{18}O$ ratios of the Karacadağ volcanic rocks are close to that for the continental subduction basalts (4.8–7.7 ‰; Hofmann et al. 1986), and bulk continental crust (8.9 ‰; Simon and Lécuyer 2005), whereas the $\delta^{18}O$ ratios of the olivine grains from the Karapınar basalts ($\delta^{18}O$ = 5.7–6.5 ‰; ESM6) have an OIB–EMII like signature (5.4–6.1 ‰; Eiler et al. 1997). Therefore, we consider that the higher $\delta^{18}O$ ratios of the Karacadağ volcanics than olivine phenocrysts from the Karapınar basalts may be attributed to the addition of $\delta^{18}O$-rich crustal components into their source or during magma evolution via assimilation of crustal material (Sun et al. 2015).

Both radiogenic Sr- and stable O-isotope ratios increase with increasing SiO_2 from basaltic to felsic rocks in the KPVF and KCVC (Figs 9a, b). Sr and O isotope ratios are then positively correlated, but they show large variations from the general trend. These are typical for crustal contamination rather than source contamination (Gertisser and Keller 2000, 2003).

To prove the crustal contamination effect in their evolution, we propose AFC and two-component mixing

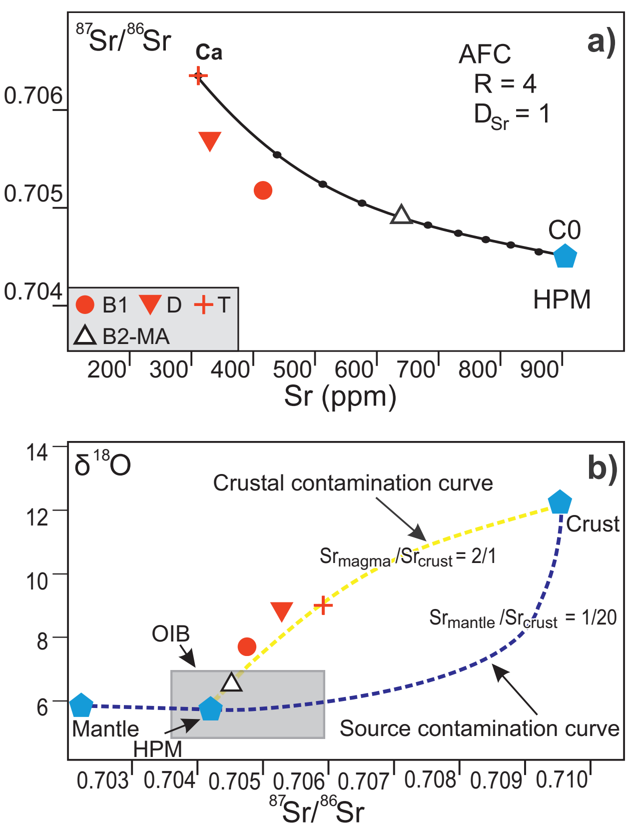

Fig. 10. a – Sr vs. $^{87}Sr/^{86}Sr$ plot for the investigated rocks displaying the assimilation–fractional crystallization (AFC) model by DePaolo (1981), **b** – $^{87}Sr/^{86}Sr$ vs. ^{18}O diagram for the rocks showing two-component mixing model, and the ratios represent Sr abundance ratios between mantle (melt when assimilation), and continental crust. R: Ratio of the assimilation rate to the fractional crystallization rate, DSr: Bulk partition coefficient of Sr, Ca: Assimilant, Co: Primary magma. Compositions of the mantle, crust and OIB were taken from Gertisser and Keller (2000). Hypothetical primary magma (HPM) composition was estimated by a data array.

models for the investigated rocks in Figs 10a and 10b. We preferred to utilize the most evolved Karacadağ unit (trachyte) as a contaminant (Ca), and used a hypothetical primary magma as C0. Fig. 10a indicates that a hypothetical primary magma (C0) could produce the mildly alkaline basalts by assimilation of the trachytes. Moreover, some of the Karapınar basalts contain sieved plagioclase, embayed and ocelli quartz, fully opacitized biotite, and amphibole xenocrysts (Fig. 3 and ESM3), which were probably plucked from the wall rock represented by the Karacadağ volcanic rocks. Investigated rocks lie along a convex–upward mixing line (Fig. 10b) confirming that both Karapınar and Karacadağ volcanics were dominantly subjected to crustal contamination during their evolution (Zhang et al. 2016; Zhiguo et al. 2018).

In the Sr–Nd isotopes diagram (Fig. 7), the area where the samples are located is represented by the interaction of sublithospheric melts with the continental lithosphere, represented by the partial melting of subducted sediments or by melts derived from the continental lithosphere. Investigated Karapınar basalts are plotted in the OIB-type rocks area. However, Karacadağ basalt deviates from the trend of Karacadağ intermediate-felsic units owing to their high positive ƐNd value (Fig. 7). Extremely high positive ƐNd values represent a long-term depleted source and also suggest that they were generated in an entirely oceanic environment devoid of the efficacy of continental crust (Dampare et al. 2009). Trace element contents and generated models indicate Karacadağ basalts were exposed to a significant crustal contamination process. Moreover, in the recent studies on CVP (Di Giuseppe et al. 2018b), the maximum value of the $^{144}Nd/^{143}Nd$ ratio is about 0.5127 of the calc-alkaline rocks in the area. Because Karacadağ basalt contains an extremely positive ƐNd value (~9) and $^{144}Nd/^{143}Nd$ ratio (0.51309), we do not prefer to use that unrealistic data to interpret the source of the rocks. Moreover, investigated rocks exhibit different areas in the Pb isotope diagrams (Fig. 8). It is possible to say that Karacadağ and Karapınar volcanic rocks may be derived from a different mantle source.

5.3. Temporal and Spatial evolution of the volcanic units

Located in the southwestern part of the CVP, the KCVC and KPVF represent volcanic episodes that occurred during the Plio–Quaternary. The KCVC was previously dated at 4.7–5.98 Ma from three samples with the K–Ar dating technique (Platzman et al. 1998), which represents the only published radiometric age data on this unit. In this study, we have dated an amphibole separate from dacites and whole-rock fragments from basalts of the KCVC with the Ar–Ar dating technique, which resulted in 5.45 and 5.65 Ma, respectively. Our new age data are in the range of the published age span, and all these suggest ~1.3 Ma duration of volcanism for the KCVC. However, the duration of volcanism in the KCVC may be more than suggested here because this interpretation is based on only five radiometric data from such a large volcanic complex. On the other hand, relatively more radiometric age data were produced from the KPVF (no age data from this study), and these indicate younger than < 0.6 Ma for the Karapınar area, but monogenetic mafic volcanism can be dated back to 2.5 Ma across the CVP (Reid et al. 2017; Dogan-Kulahci et al. 2018; Notsu et al. 1995).

The published ages from the Cappadocia Volcanic Province (CVP) range from ~14 Ma to recent times and show obvious spatial, temporal and geochemical variations of volcanic activity in the province. The CVP extends in NE–SW direction, and vent alignments of the volcanoes in the CVP are mainly NE–SW to N–S (Toprak 1998; Higgings et al. 2015). The main geochemical and spatiotemporal characteristics of the CVP are that the Late Miocene to Pliocene volcanic rocks are mainly calc–alkaline. Still, the Plio–Quaternary volcanic rocks are calc–alkaline or (mildly) Na-alkaline in compositions, both of which have orogenic geochemical signature and southwest-ward younging of the volcanism (see section 2 for references). Schleiffarth et al. (2018) and Reid et al. (2017) argued that the SW younging age progression seen in the CVP could be related to the steepening and rollback of the Cyprean slab beneath the Kırşehir and Central Anatolide–Tauride Blocks, causing upwelling asthenospheric mantle. On the other hand, most authors suggested that geochemical characteristics of the CVP resulted from extension-related melting and the Late Miocene to Pliocene calc-alkaline volcanic rocks were derived from the subduction-modified lithospheric mantle. But, the origin of the Plio–Quaternary mafic to intermediate volcanic rocks displaying (mildly) Na-alkaline to calc–alkaline geochemical character is still controversial. Ignoring the crustal contamination, Di Giuseppe et al. (2018b) proposed a petrologic model including mixing between different percentages of within-plate (OIB)-like magmas derived from the sub-lithospheric mantle and calc–alkaline magmas from subduction-modified lithospheric mantle for the origin of the Plio–Quaternary Na-alkaline basalts in the CVP. However, such a model may not be possible for the KPVF basalts because they show evidence of crustal contamination discussed in section 5.2. Thus, we suggest that the KPVF basaltic magmas, originally of anorogenic geochemical signature, interacted with the upper crustal component represented by the KCVC via AFC-style differentiation to gain an orogenic signature. A similar model was suggested by Kocaarslan and Ersoy (2018) for the Kangal–Gürün Basin volcanic rocks located to the east of the CVP. In this model, they argued that orogenic geochemical signature could result from crustal contamination of originally anorogenic magmas derived from an upwelling mantle source unmodified by any subduction-related metasomatism. Although having OIB-like signatures in terms of radiogenic and stable isotope ratios and trace element contents, Karapınar basalts show a trend extending in the region between OIB and continental crust in the SiO_2 *vs.* Nb/U and Ce/Pb diagrams (ESM5). The reported evidence suggests that the crustal contamination signature decreased from calc–alkaline to mildly-alkaline basalts from the Mio–Pliocene to the Quaternary. However, in the Quaternary, raised in the evolution of the basalts from mildly-alkaline (B2-MA) to calc–alkaline (B2-CA, B3) (ESM1, ESM2, ESM5).

6. Conclusions

The petrographical, geochemical, and geochronological data obtained from this and previous studies have allowed us to put the following constraints regarding the evolution and origin of the Karacadağ Volcanic Complex and Karapınar Volcanic Field.

a) The Karacadağ volcanic complex is represented by basaltic to dacitic and trachytic rocks that erupted during the late Miocene–Pliocene, showing calc–alkaline affinity. Our Ar–Ar geochronology analysis yielded ages from 5.45 to 5.65 Ma, representing a short time interval of the longer-lasted Karacadağ volcanism deduced from the published age data. Similar to orogenic volcanic rocks, the isotopic and geochemical characteristics of the basaltic Karacadağ volcanic rocks suggest their derivation from parental magmas generated in a subduction-modified lithospheric mantle. The suite's intermediate and felsic rock types evolved by fractional crystallization plus crustal contamination and magma mixing to a lesser extent.
b) The Karapınar volcanic rocks ranging from basalt to andesite erupted during Quaternary and are characterized by both mildly alkaline and calc–alkaline compositions. Trace element geochemistry of the Karapınar basaltic rocks is similar to those of orogenic volcanic rocks as in the Karacadağ basaltic rocks, whereas their ^{18}O values are in the range of OIB-like rocks.
c) Presence of crustal xenoliths and xenocrysts derived from the Karacadağ rocks, and isotopic variations in the Karapınar basalts indicate that crustal contamination had a key role in their evolution, and this process is responsible for the obtaining orogenic signature of the OIB-like Karapınar basalts.
d) Taken as a whole, the obtained data can be elucidated by the derivation of the Karapınar basaltic rocks from an OIB-like mantle source and then contamination with the Karacadağ volcanic rocks at a shallow crustal level. This may be an alternative model for explaining orogenic geochemical signature in sodic alkali basalts in the CVP.

Acknowledgments This study was financially supported by Tübitak Çaydag project number 118Y252 and Selcuk University Bap project number 17401117. We thank Professor Yusuf Kağan Kadıoğlu and Dr. Kıymet Deniz for making the thin sections. The authors thank to the Handling Editor Dr. Vladislav Rapprich, and Professor Tamer Koralay, Dr. Raymundo Casas-García, and an anonymous reviewer for their critical and constructive comments that improved the quality of this paper.

Electronic supplementary material. Supplementary data for this paper are available online at the Journal web site (http://dx.doi. org/10.3190/jgeosci.343).

References

Aldanmaz E (2002) Mantle Source Characteristics of Alkali Basalts and Basanites in an Extensional Intracontinental Plate Setting, Western Anatolia, Turkey: Implications for Multi-stage Melting. Int Geol Rev 44: 440–457

Aldanmaz E, Pearce JA, Thirlwall MF, Mitchell JG (2000) Petrogenetic evolution of late Cenozoic, post-collision volcanism in western Anatolia, Turkey. J Volcanol Geotherm Res 102: 1–2: 67–95

Aydar E, Schmitt AK, Çubukçu HE, Akin L, Ersoy O, Sen E, Duncan RA, Atici G (2012) Correlation of ignimbrites in the central Anatolian volcanic province using zircon and plagioclase ages and zircon compositions. J Volcanol Geotherm Res 213: 83–97

Aydar E, Cubukcu HE, Şen E, Akin L (2013) Central Anatolian Plateau, Turkey: incision and paleoaltimetry recorded from volcanic rocks. Turkish J Earth Sci 22, 5: 739–746

Baker J, Peate D, Waight T, Meyzen C (2004) Pb isotopic analysis of standards and samples using a ^{207}Pb–^{204}Pb double spike and thallium to correct for mass bias with a double-focusing MC-ICP-MS. Chem Geol 211, 3–4: 275–303

Batum I (1978) Geology and petrography of Acıgöl and Göllüdağ volcanics at SW of Nevşehir, Central Anatolia, Turkey. Geosciences 4: 50–69

Besang C, Echardt FJ, Harre W, Kreuzer H, Müller P (1977) Radiometrische Altersbestimmungen an neogenen Eruptivgesteinen der Turkei. Geol Jahrb B25: 3–36

Bigazzi G, Yegingil Z, Ercan T, Oddone M, Özdogan M (1993) Fission track dating obsidians in Central and Northern Anatolia. Bull Volcanol 55, 8: 588–595

Biryol CB, Beck SL, Zandt G, Özacar AA (2011) Segmented African lithosphere beneath the Anatolian region inferred from teleseismic P-wave tomography. Geophys J Int 184, 3: 1037–1057

Bonin B (2004) Do coeval mafic and felsic magmas in post-collisional to within-plate regimes necessarily imply two contrasting, mantle and crustal, sources? A review. Lithos 78: 1–24

Bryan WB, Finger LW, Chayes F (1969) Estimating Proportions in Petrographic Mixing Equations by Least-Squares Approximation. Science 163, 3870: 926–927

Clayton RN, Mayeda TK (1963) The use of bromine pentafluoride in the extraction of oxygen from oxides and silicates for isotopic analysis. Geochim Cosmochim Acta 27, 1: 43–52

Cosentino D, Schildgen TF, Cipollari P, Faranda C, Gliozzi E, Hudáčková N, Lucifora S, Strecker MR (2012) Late Miocene surface uplift of the southern margin of the Central Anatolian Plateau, Central Taurides, Turkey. Bulletin 124, 1–2: 133–145

Dai LQ, Zheng F, Zhao ZF, Zheng YF (2018) Geochemical insights into the lithology of mantle sources for Cenozoic alkali basalts in West Qinling, China. Lithos 302–303: 86–98

Dampare S, Shibata T, Asiedu D, Okano O, Manu J, Sakyi P (2009) Sr–Nd isotopic compositions of Paleoproterozoic metavolcanic rocks from the southern Ashanti volcanic belt, Ghana. Okayama Univ Earth Sci Rep 16, 1: 9–28

Davidson JP, Harmon RS (1989) Oxygen isotope constraints on the petrogenesis of volcanic arc magmas from Martinique, Lesser Antilles. Earth Planet Sci Lett 95, 3: 255–270

Davidson J, Wilson M (2011) Differentiation and Source Processes at Mt Pelée and the Quill; Active Volcanoes in the Lesser Antilles Arc. J Petrol 52, 7–8: 1493–1531

Davidson J, Turner S, Handley H, Macpherson C, Dosseto A (2007) Amphibole “sponge” in arc crust? Geology 35, 9: 787–790

Depaolo DJ (1981) Trace element and isotopic effects of combined wallrock assimilation and fractional crystallization. Earth Planet Sci Lett 53, 2: 189–202

Di giuseppe P, Agostini S, Lustrino M, Karaoğlu Ö, Savaşçin MY, Manetti P, Ersoy Y (2018a) Transition from Compression to Strike-slip Tectonics Revealed by Miocene–Pleistocene Volcanism West of the Karlıova Triple Junction (East Anatolia). J Petrol 58, 10: 2055–2087

Di giuseppe P, Agostini S, Manetti P, Savaşçin MY, Conticelli S (2018b) Sub-lithospheric origin of Na-alkaline and calc-alkaline magmas in a post-collisional tectonic regime: Sr–Nd–Pb isotopes in recent monogenetic volcanism of Cappadocia, Central Turkey. Lithos 316–317: 304–322

Dobosi G, Downes H, Mattey D, Embey-isztin A (1998) Oxygen isotope ratios of phenocrysts from alkali basalts of the Pannonian basin: Evidence for an O-isotopically homogeneous upper mantle beneath a subduction-influenced area. Lithos 42: 213–223

Dogan-kulahci GD, Temel A, Gourgaud A, Varol E, Guillou H, Deniel C (2018) Contemporaneous alkaline and calc-alkaline series in Central Anatolia (Turkey): Spatio-temporal evolution of a post-collisional Quaternary basaltic volcanism. J Volcanol Geotherm Res 356: 56–74

Downes H, Pantó G, Póka T, Mattey D, Greenwood PB (1995) Calc-alkaline volcanics of the Inner Carpathian arc, Northern Hungary: New geochemical and oxygen isotopic results. Acta Vulcanol 7: 29–41

Eiler JM, Farley KA, Valley JW, Hauri E, Craig H, Hart SR, Stolper EM (1997) Oxygen isotope variations in ocean island basalt phenocrysts. Geochim Cosmochim Acta 61, 11: 2281–2293

Ellam RM, Harmon RS (1990) Oxygen isotope constraints on the crustal contribution to the subduction-related magmatism of the Aeolian Islands, southern Italy. J Volcanol Geotherm Res 44, 1: 105–122

Ercan T, Fujitami T, Matsuda J, Tokel S, Notsu K (1990) Origin and Evolution of the Cenozoic aged Volcanism around Hasandağı–Karacadağ (Central Anatolia). J Geomorph 18: 39–54

Ercan T, Tokel S, Matsuda J, Ui T, Notsu K, Fujitani T (1992) New geochemical, isotopic and radiometric data of the Quaternary volcanism of Hasandağı–Karacadağ (Central Anatolia). TJK Bull 7: 8–21 (in Turkish with English abstract)

Ersoy YE, Helvaci C, Palmer MR (2012) Petrogenesis of the Neogene volcanic units in the NE–SW-trending basins in western Anatolia, Turkey. Contrib Mineral Petrol 163, 3: 379–401

Faccenna C, Becker TW, Lucente FP, Jolivet L, Rossetti F (2001) History of subduction and back arc extension in the Central Mediterranean Geophys J Int 145, 3: 809–820

Faccenna C, Bellier O, Martinod J, Piromallo C, Regard V (2006) Slab detachment beneath eastern Anatolia: A possible cause for the formation of the North Anatolian fault. Earth Planet SciLett 242, 1–2: 85–97

Geldmacher J, Hoernle K, Klügel A, Bogaard P, Wombacher F, Berning B (2006) Origin and geochemical evolution of the Madeira–Tore Rise (eastern North Atlantic). J Geophys Res: Solid Earth 111: B09206

Gertisser R, Keller J (2000) From basalt to dacite: origin and evolution of the calc–alkaline series of Salina, Aeolian Arc, Italy. Contrib Mineral Petrol 139, 5: 607–626

Gertisser R, Keller J (2003) Trace Element and Sr, Nd, Pb and O Isotope Variations in Medium-K and High-K Volcanic Rocks from Merapi Volcano, Central Java, Indonesia: Evidence for the Involvement of Subducted Sediments in Sunda Arc Magma Genesis. J Petrol 44, 3: 457–489

Govers R, Wortel M (2005) Lithosphere tearing at STEP faults: Response to edges of subduction zones. Earth Planet Sci Lett 236, 1–2: 505–523

Güleç N (1991) Crust–mantle interaction in western Turkey: implications from Sr and Nd isotope geochemistry of Tertiary and Quaternary volcanics. Geol Mag 128, 5: 417–435

Harangi S, Downes H, Seghedi I (2006) Tertiary–Quaternary subduction processes and related magmatism in the Alpine–Mediterranean region. Geological Society London, Memoirs 32: 167–190

Higgins M, Schoenbohm LM, Brocard G, Kaymakci N, Gosse JC, Cosca MA (2015) New kinematic and geochronologic evidence for the Quaternary evolution of the Central Anatolian fault zone (CAFZ). Tectonics 34, 10: 2118–2141

Hoernle K, Tilton G, Schmincke HU (1991) Sr-Nd-Pb isotopic evolution of Gran Canaria: Evidence for shallow enriched mantle beneath the Canary Islands. Earth Planet Sci Lett 106, 1–4: 44–63

Hofmann AW (1986) Nb in Hawaiian magmas: Constraints on source composition and evolution. Chem Geol 57, 1–2: 17–30

Hofmann AW (1988) Chemical differentiation of the Earth: the relationship between mantle, continental crust, and oceanic crust. Earth Planet Sci Lett 90, 3: 297–314

Hofmann AW (1997) Mantle Geochemistry: The Message from Oceanic Volcanism. Nature 385, 6613: 219–229

Hofmann AW (2007) Sampling Mantle Heterogenity through Oceanic Basalts: Isotopes and Trace Elements. In: H.D. Holland and K.K. Turekian (Editors), Treatise on Geochemistry. Pergamon, Oxford, pp 1–44

Hofmann AW, Jochum KP, Seufert M, White WM (1986) Nb and Pb in oceanic basalts: new constraints on mantle evolution. Earth Planet Sci Lett 79, 1–2: 33–45

Innocenti F, Mazzuoli R, Pasquarè G, Radicati Di Brozolo F, Villari L (1975) The Neogene calcalkaline volcanism of Central Anatolia: geochronological data on Kayseri-Nigde area. Geol Mag 112, 4: 349–360

Innocenti F, Agostini S, Di vincenzo G, Doglioni C, Manetti P, Savaşçin MY, Tonarini S (2005) Neogene and Quaternary volcanism in Western Anatolia: Magma sources and geodynamic evolution. Marine Geol 221, 1: 397–421

Irvine T, Baragar WRA (1971) A Guide to the Chemical Classification of the Common Volcanic Rocks. Can J Earth Sci 8: 523–548

Jung S, Pfänder JA, Brauns M, Maas R (2011) Crustal contamination and mantle source characteristics in continental intra-plate volcanic rocks: Pb, Hf and Os isotopes from central European volcanic province basalts. Geochim Cosmochim Acta 75, 10: 2664–2683

Keller J (1974) Quaternary Maar Volcanism near Karapınar in Central Anatolia. Bull Volcanol 38, 1: 378–396

Kheirkhah M, Neill I, Allen MB (2015) Petrogenesis of OIB-like basaltic volcanic rocks in a continental collision zone: Late Cenozoic magmatism of Eastern Iran. J Asian Earth Sci 106: 19–33

Kocaarslan A, Ersoy EY (2018) Petrologic evolution of Miocene–Pliocene mafic volcanism in the Kangal and Gürün basins (Sivas–Malatya), central east Anatolia: Evidence for Miocene anorogenic magmas contaminated by continental crust. Lithos 310–311: 392–408

Kretz R (1983) Symbols for rock-forming minerals: Am Mineral: 68: 1–2: 277–279

Le bas MJ, Le maitre RW, Streckeisen A, Zanettin BA (1986) A Chemical Classification of Volcanic Rocks Based on the Total Alkali–Silica Diagram. J Petrol 127: 745

Le pennec JL, Temel A, Froger JL, Sen S, Gourgaud A, Bourdier JL (2005) Stratigraphy and age of the Cappadocia ignimbrites, Turkey: reconciling field constraints with paleontologic, radiochronologic, geochemical and paleomagnetic data. J Volcanol Geotherm Res 141, 1–2: 45–64

Lepetit P, Viereck L, Piper JDA, Sudo M, Gürel A, Çopuroğlu I, Gruber M, Mayer B, Koch M, Tatar O, Gürsoy H (2014) $^{40}Ar/^{39}Ar$ dating of ignimbrites and plinian air-fall layers from Cappadocia, Central Turkey: Implications to chronostratigraphic and Eastern Mediterranean palaeoenvironmental record. Geochemistry 74, 3: 471–488

Lustrino M, Wilson M (2007) The circum-Mediterranean anorogenic Cenozoic igneous province. Earth-Sci Rev 81, 1–2: 1–65

Münker C, Pfänder JA, Weyer S, Büchl A, Kleine T, Mezger K (2003) Evolution of planetary cores and the Earth-Moon system from Nb/Ta systematics. Science 301, 5629: 84–87

Notsu K, Fujitani T, Ui T, Matsuda J, Ercan T (1995) Geochemical features of collision-related volcanic rocks in central and eastern Anatolia, Turkey. J Volcanol Geotherm Res:64, 3: 171–191

Okay AI (2008) Geology of Turkey: A Synopsis. Anschnitt 21: 19–42

Okay AI, Tüysüz O (1999) Tethyan sutures of northern Turkey. In: Durand B, Jolivet L, Hovarth F, Séranne M (eds) The Mediterranean Basins: Tertiary Extension within the Alpine Orogen. Geological Society London, Special Publication 156, pp 475–515

Olanca K (1999) Quaternary Volcanism of Karapınar-Konya Region: Geohemical Evaluation. Geosciences 21: 115–124 (in Turkish with English asbtract)

Pearce JA (1983) Role of the sub-continental lithosphere in magma genesis at active continental margins. In: Hawkesworth CJ, Norry MJ (eds) Continental Basalts and Mantle Xenoliths. Cambridge, Shiva Pub Ltd., pp 230–249

Pearce J (1996) A user's guide to basalt discrimination diagrams: Trace Element Geochemistry of Volcanic Rocks: Applications for Massive Sulphide Exploration. Geological Association of Canada Short Course Notes.: 79–113

Pearce JA, Peate DW (1995) Tectonic Implications of the Composition of Volcanic ARC Magmas. Ann Rev Earth Planet Sci 23, 1: 251–285

Pearce JA, Bender JF, De long SE, Kidd WSF, Low PJ, Güner Y, Saroglu F, Yilmaz Y, Moorbath S, Mitchell JG (1990) Genesis of collision volcanism in Eastern Anatolia, Turkey. J Volcanol Geotherm Res 44, 1: 189–229

Peccerillo A, Dallai L, Frezzotti ML, Kempton PD (2004) Sr–Nd–Pb–O isotopic evidence for decreasing crustal contamination with ongoing magma evolution at Alicudi volcano (Aeolian arc, Italy): implications for style of magma-crust interaction and for mantle source compositions. Lithos 78, 1: 217–233

Pfänder JA, Jung S, Münker C, Stracke A, Mezger K (2012) A possible high Nb/Ta reservoir in the continental lithospheric mantle and consequences on the global Nb budget – Evidence from continental basalts from Central Germany. Geochim Cosmochim Acta 77: 232–251

Platzman ES, Tapirdamaz C, Sanver M (1998) Neogene anticlockwise rotation of central Anatolia (Turkey): preliminary palaeomagnetic and geochronological results. Tectonophysics 299, 1: 175–189

Rabayrol F, Hart CJR, Thorkelson DJ (2019) Temporal, spatial and geochemical evolution of late Cenozoic post-subduction magmatism in central and eastern Anatolia, Turkey. Lithos 336–337: 67–96

Reid MR, Schleiffarth WK, Cosca MA, Delph JR, Blichert-toft J, Cooper KM (2017) Shallow melting of MORB-like mantle under hot continental lithosphere, Central Anatolia. Geochem Geophys Geosyst 18, 5: 1866–1888

Rudnick R, Gao S (2003) Composition of the Continental Crust. Treatise Geochem 3: 1–64

Schildgen TF, Cosentino D, Bookhagen B, Niedermann S, Yildirim C, Echtler H, Wittmann H, Strecker MR (2012) Multi-phased uplift of the southern margin of the Central Anatolian plateau, Turkey: A record of tectonic and upper mantle processes. Earth Planet Sci Lett 317: 85–95

Schleiffarth W, Darin M, Umhoefer P, Reid M (2018) Dynamics of episodic Late Cretaceous–Cenozoic magmatism across Central to Eastern Anatolia: New insights from an extensive geochronology compilation. Geosphere 14, 5: 1990–2008

Şengör AMC, Özeren S, Genç T, Zor E (2003) East Anatolian high plateau as a mantle-supported, north–south shortened domal structure. Geophys Res Lett 30, 24: 8045

Şengör AMC, Lom N, Sunal G, Zabci C, Sancar T (2019) The phanerozoic palaeotectonics of Turkey. Part I: an inventory: Mediterranean. Geoscience Rev 1, 1: 91–161

Simon L, Lécuyer C (2005) Continental recycling: The oxygen isotope point of view. Geochem Geophs Geosys 6.8

Sun S, Mcdonough W (1989) Chemical and isotopic systematics of oceanic basalts: implications for mantle composition and processes. Geological Society, London, Special Publications, 42, 1: 313–345

Sun Y, Ying J, Su B, Zhou X, Shao J (2015) Contribution of crustal materials to the mantle sources of Xiaogulihe ultrapotassic volcanic rocks, Northeast China: New constraints from mineral chemistry and oxygen isotopes of olivine. Chem Geol 405: 10–18

Temel A, Gündoğdu MN, Gourgaud A, Le pennec JL (1998) Ignimbrites of Cappadocia (Central Anatolia, Turkey): Petrology and Geochemistry. J Volcanol Geotherm Res 85, 1–4: 447–471

Toprak V (1998) Vent distribution and its relation to regional tectonics, Cappadocian Volcanics, Turkey. J Volcanol Geotherm Res 85, 1: 55–67

Ulu Ü (2009) Geological Maps of Turkey Karaman-M30 Sheet. General Directorate of Mineral Research and Exploration, Ankara (in Turkish)

Uslular G, Gençalioğlu-kuşcu G (2019) Mantle source heterogeneity in monogenetic basaltic systems: A case study of Eğrikuyu monogenetic field (Central Anatolia, Turkey). Geosphere 15, 2: 295–323

Whitney DL, Evans BW (2009) Abbreviations for names of rock-forming minerals: Amer Miner 95, 1: 185–187

Wilson M, Bianchini G (1999) Tertiary–Quaternary magmatism within the Mediterranean and surrounding regions Geological Society London, Special Publication 156, 1: 141–168

Zhang D, Zhang Z, Mao J, Huang H, Cheng Z (2016) Zircon U–Pb ages and Hf–O isotopic signatures of the Wajilitag and Puchang Fe–Ti oxide-bearing intrusive complexes: Constraints on their source characteristics and temporal-spatial evolution of the Tarim large igneous province. Gondwana Res 37: 71–85

Zhiguo C, Xie Q, Hou T, Ke S (2018) Subducted slab-plume interaction traced by magnesium isotopes in the northern margin of the Tarim Large Igneous Province. Earth Planet Sci Lett 489: 100–110

Zindler A, Hart SR (1986) Chemical Geodynamics. Ann Rev Earth Planet Sci 14: 493–571